separations

MDPI

Article

Separation and Purification of Taxanes from Crude *Taxus cuspidata* Extract by Antisolvent Recrystallization Method

Yajing Zhang, Zirui Zhao, Wenlong Li, Yuanhu Tang, Huiwen Meng and Shujie Wang *

College of Biological and Agricultural Engineering, Jilin University, Changchun 130022, China
* Correspondence: wangshujie132@163.com

Abstract: Taxanes are natural compounds with strong antitumor activity. In this study, we first enriched taxanes by ultrasonic extraction and liquid–liquid extraction from *Taxus cuspidata*, then purified these taxanes by the antisolvent recrystallization method, and discussed the effects of four recrystallization conditions on the purity of eight target compounds. The most promising purification results were obtained using methanol as a solvent and water as an antisolvent. Response surface methodology (RSM) was used to further optimize the optimal purification conditions: when the crude extraction concentration was 555.28 mg/mL, an antisolvent to solvent volume ratio was 28.16 times, the deposition temperature was 22.91 °C, and the deposition time was 1.76 min, the purity of the taxanes reached its maximum. The scanning electron microscopy (SEM) results showed that recrystallization could effectively reduce the particle size of crude *Taxus cuspidata* and control the particle morphology. X-ray diffraction (XRD) and Raman spectrum experiments demonstrated that the amorphous state of the crude *Taxus cuspidata* did not change during the recrystallization process, and always remained amorphous. This recrystallization method can effectively improve the purity of taxanes in *Taxus cuspidata*, and is suitable for the preliminary purification of taxanes.

Keywords: taxanes; *Taxus cuspidata*; antisolvent recrystallization method; SEM; XRD; Raman spectrum

Citation: Zhang, Y.; Zhao, Z.; Li, W.; Tang, Y.; Meng, H.; Wang, S. Separation and Purification of Taxanes from Crude *Taxus cuspidata* Extract by Antisolvent Recrystallization Method. *Separations* **2022**, *9*, 304. https://doi.org/10.3390/separations9100304

Academic Editor: Paraskevas D. Tzanavaras

Received: 13 September 2022
Accepted: 9 October 2022
Published: 11 October 2022

1. Introduction

Taxus plants are evergreen trees or shrubs of Taxaceae, and there are approximately 11 species in the world [1–3]. Wild resources of *Taxus* are scarce, and it has unique medicinal value. It has been recorded in "Materia Medica Tuixin" that *Taxus* can be used as a medicine, and has the effects of diuresis, dredging channels, bacteriostasis, detoxification, anti-inflammation and detoxification, and can treat kidney disease, diabetes, oral ulcers, uterine fibroids, rheumatoid diseases, and other diseases [4]. Furthermore, *Taxus* can also improve human immunity, restore human natural functions, and reduce the loss of protein [5].

Taxus cuspidata is a kind of *Taxus* plant, mainly distributed across the Changbai Mountain (China), Japan, and Korea [6–8]. *Taxus cuspidata* has complex components including taxane diterpenoids, sesquiterpenes, steroids, lignans, flavonoids, glycosides, and other compounds [9–14]. Its stems and leaves contain paclitaxel (PTX), which is a valuable secondary metabolite with important medical value [15–18]. Aside from paclitaxel, *Taxus cuspidata* contains other taxane diterpenoids [19–21]. However, the yield of taxanes in *Taxus cuspidata* is very low, so it is difficult to separate and purify them [22,23]. Furthermore, the structure of taxanes is unstable, and it is easily isomerized and degraded under the influence of acid, alkali, and temperature. In addition, because the structures of taxanes are similar, it is even more difficult to separate and purify them [24]. The effective separation and purification of taxanes in *Taxus cuspidata* have important research significance, and it is therefore necessary to comprehensively and deeply explore the separation and purification of paclitaxel to establish a rapid, efficient, economical, and environmentally friendly separation and purification method.

Among the various purification methods for taxanes, the most commonly used are column chromatography, macroporous resin, molecular imprinting, recrystallization, and chromatography [25–33]. At present, the separation and purification of taxanes mainly focuses on column chromatography. However, according to previous research and analysis, if column chromatography is used to experimentally purify taxanes, it will take a long time, and some products will be lost while passing through the column. Moreover, the molecular weights of taxanes are close, so it is difficult to separate them by column chromatography [34]. Therefore, it is necessary to explore a low-cost and environmentally friendly extraction and purification method.

The recrystallization method can make use of the different solubilities of the components in the mixture in a certain solvent or at different temperatures in the same solvent in order to separate them from each other [35–37]. Taxanes are soluble in organic solvents such as methanol, but insoluble in petroleum ether, n-hexane, and water [38]. Therefore, methanol was used as solvent; petroleum ether, n-hexane, and water as the antisolvent; and paclitaxel was preliminarily purified.

Wang et al. purified ellagic acid from pomegranate peel by extraction, acid hydrolysis, and antisolvent recrystallization. Response surface methodology based on five-level and four-variable central composite design was used to find the best purification conditions [39]. Zhao et al. used ethanol as the solvent and n-hexane as the antisolvent to improve the content of flavonoids in the *Ginkgo biloba* extract by antisolvent recrystallization [40]. Tarbe M et al. purified aconitine from aconitum by recrystallization, a method that can avoid the degradation of aconitine [41].

Response surface methodology (RSM) is a widely used mathematical and statistical technique for modeling and optimizing the process for the extraction of bioactive compounds. Other such methods include conventional solvent extraction (CSE), microwave-assisted extraction (MAE), supercritical fluid extraction (SFE), and ultrasound-assisted extraction (UAE) [42]. Wu et al. applied the RSM to investigate the effects of three independent variables including ethanol concentration (%), extraction time (min), and solvent-to-material ratio (mL/g) on the ultrasound-assisted extraction (UAE) of phenolics from Flos Chrysanthemi (FC). The data suggest that the optimal UAE condition was an ethanol concentration of 75.3% and extraction time of 43.5 min, whereas the ratio of solvent to material had no significant effect. When the free radical scavenging ability was used as an indicator of a successful extraction, a similar optimal extraction was achieved with an ethanol concentration of 72.8%, extraction time of 44.3 min, and ratio of solvent to material of 29.5 mL/g [43]. Tian et al. used RSM to study three extraction parameters: extraction time, solid–liquid ratio, and extraction temperature. The results showed that the optimum extraction conditions of the pilot plant extraction process of 1-deoxynojirimycin (1-DNJ) were an extraction temperature of 79.2 degrees C, extraction time of 1.46 h (87.6 min), and ratio of sample to solvent of 1:9.82. Under these optimum conditions, the extraction yield was found to be 31.62 mg/g [44]. Kwak et al. used RSM to predict the optimum conditions for the estrogenic activity of the Rheum undulatum extract. A Box–Behnken design was used to monitor the effect of ethanol concentration, extraction temperature, and extraction time. Optimum extraction conditions were predicted to be 57.1%, 65.2 °C, and 23.6 h. The experimental value found for estrogenic activity was 1.90 ± 0.1, which agreed with the predicted value of 1.95 [45].

In the present study, we aimed to establish an efficient purification method for taxanes from *Taxus cuspidata*. Our data showed that the Box–Behnken design (BBD) and RSM model verified the reliability of the antisolvent recrystallization purification method. A scanning electron microscope (SEM) was used to compare the morphological changes before and after purification. The XRD and Raman spectra were used to detect and analyze the crystal form and structure of the crude and recrystallized products of *Taxus cuspidata*. The purity of taxanes in *Taxus cuspidata* increased from the initial 0.20% to 23.238%, with the purity of purified taxanes being 116.19 times that of the original, which was suitable for the large-scale preliminary purification of taxanes.

2. Materials and Methods

2.1. Materials and Reagents

Taxus cuspidata needles were plucked from a ten-year-old *Taxus cuspidata* specimen planted in the experimental field of the College of Biological and Agricultural Engineering, Jilin University (Jilin, China).

Chromatographic-grade acetonitrile and chromatographic-grade methanol were purchased from the American Tedia Company (Cincinnati, OH, USA). Ethanol, ethyl acetate, n-hexane, petroleum ether as well as all the above reagents were of analytical grade (Shanghai, China). Purified water was produced by the Hangzhou Wahaha Company (Hangzhou, China). Paclitaxel (PTX), 10-deacetylbaccatin III (10-DAB III), baccatin III (BAC III), 7-xylogan-10-deacetyltaxol (DXT), docetaxel (DOT), 7-epitaxol (7-EPT), cephalomannine (CEPH), and 10-deacetyltaxol (10-DAT) with a purity >98% were bought from Shanghai Yuanye Bio-Technology Co. Ltd. (Shanghai, China).

2.2. Ultrasonic Extraction and Liquid–Liquid Extraction

In this paper, ethanol was initially selected as the extraction solvent, and then liquid–liquid extraction was carried out on the extract. The extractant was ethyl acetate. The needles of *Taxus cuspidata* were dried in an oven at 40 °C to constant weight, then fully ground, and a certain volume of ethanol solution was added for the ultrasonic extraction test [46]. After extraction, the supernatant was centrifuged, poured into a rotary evaporator and evaporated to dryness, and to the mixture was added ethyl acetate:water in a ratio of 1:1. The suspension was placed in a separatory funnel, left to stand, and layered to obtain an organic phase, and an equal volume was added to the aqueous phase. The aqueous phase was extracted three times, the obtained organic phase solutions were mixed, and the organic solvent was recovered by vacuum concentration. The concentrate was dried in an oven at 40 °C to obtain a brown solid extract, which was accurately weighed. A small amount of the extract was fully dissolved in methanol, and filtered by a 0.22 μm organic microporous membrane, and the purity of taxanes was detected by high-performance liquid chromatography (HPLC).

2.3. Selection of Antisolvent for Recrystallization

The necessary volume of methanol was added to dissolve three solid extracts of *Taxus cuspidata*, and then a certain volume of n-hexane, petroleum ether, and water, respectively, was added. Samples were placed in an ultrasound to fully mix them before being centrifuged at 5000 rpm for 10 min. Then, the precipitate was collected, dried in a drying box at 40 °C, and accurately weighed. A small amount of solid powder was taken, fully dissolved in methanol, and filtered with a 0.22 μm organic microporous membrane, and then the purity of taxanes was detected by HPLC.

$$\text{Taxanes purity} = (\text{Taxane yields in } \textit{Taxus cuspidata})/(\textit{Taxus cuspidata} \text{ total amount}) \times 100\%$$

$$\text{Recovery rate of taxanes} = (\text{Taxane yields after purification})/(\text{Taxane yields before purification}) \times 100\%$$

2.4. Single-Factor Experiment

Because there are many factors affecting the purity of taxanes in *Taxus cuspidata*, a single-factor experiment was designed and carried out. The experimental ranges of the different factors used in this study were as follows: a crude extraction concentration of 100–600 mg/mL, an antisolvent to solvent volume ratio of 5–30 times, a deposition temperature of 20–45 °C, and a deposition time of 1–11 min.

2.5. RSM Experiment

Four factors—crude extraction concentration (X_1), antisolvent to solvent volume ratio (X_2), deposition temperature (X_3) and deposition time (X_4)—were selected as dependent variables in the single-factor experiment, and the purity of taxanes was used as the response

value. The Box–Behnken design (BBD) assay was adopted to optimize the four dependent variables on the basis of four factors and three levels. There were 29 sets of experiments, and each set of experiments was repeated three times.

The data-processing system of Design Expert12 (V12.0.3.0, Stat-Ease Inc., Minneapolis, MN, USA) was used for statistics, and curve-fitting was performed using the Origin Pro2021 software (V9.8.0.200, OriginLab Corporation, Northampton, MA, USA).

2.6. HPLC Detection of Taxane Yields

The yields of each taxane in the extract were quantified by high-performance liquid chromatography (HPLC, UltiMate 3000 Separations Module, Waltham, MA, USA). The gradient elution procedure was set as follows: Inertsil ODS-3 C18 column (250 mm × 4.6 mm, 5 μm), column temperature 30 °C. The detection wavelength was 227 nm; the flow rate was 0.8 mL/min; the injection volume was 10 μL; and the mobile phase A was water and B was acetonitrile. The gradient elution procedure was as follows: at 0–10 min, B increased from 40% to 50%, and at 10–13 min, B increased from 50% to 53%. At 13–25 min, B increased from 53% to 73%, and at 25–30 min, B decreased from 73% to 40% for 10 min.

To generate the mixed standard curve, a total of 10 mg of paclitaxel (PTX), 10-deacetyltaxol (10-DAT), baccatin III (BAC III), 10-deacetylbaccatin III (10-DAB III), 7-xylogan-10-deacetyltaxol (DXT), cephalomannine (CEPH), docetaxel (DOT), and 7-epitaxol (7-EPT) standard were accurately weighed and dissolved in methanol to a constant volume of 10 mL. Then, the samples were diluted with methanol to prepare solutions with different concentration gradients. The peak areas of standard solutions with different concentrations were measured by high-performance liquid chromatography at 227 nm, and the high-performance liquid standard curves of eight standards were drawn with the standard concentration as the abscissa and the peak area as the ordinate [46]. The concentrations of eight taxanes were calculated using the calibration curves. The total yield of the eight main taxanes of *Taxus cuspidata* was calculated as follows:

$$\text{Taxane yields} = C \times V/W$$

where C (μg/mL) is the total content of eight main taxanes; V (mL) is the volume of extraction solution recovered; and W (g) is the weight of *Taxus cuspidata*.

2.7. SEM

The microstructure of the *Taxus cuspidata* products before and after recrystallization was observed using a Sigma300 ultra-low temperature scanning electron microscope (Oberkochen, Germany). A small amount of *Taxus cuspidata* powder was taken before and after recrystallization and purification, stuck to conductive adhesive, sprayed gold by ion sputtering, observed, and photographed with a scanning electron microscope.

2.8. XRD

With the D8 ADVANCE X-ray diffractometer (Karlsruhe, Germany), the tube pressure is 40 MA, the target is Cu, the scanning speed is 5°/min, the scanning range is 5–60, and the step width is 0.05. The crude and recrystallized products of *Taxus cuspidata* were detected, respectively.

2.9. Raman Spectrum

The crude and recrystallized products of *Taxus cuspidata* were placed on a glass slide, in which the solid powder sample needs to be flattened and placed on a microscope stage to detect the Raman signal using a HORIBA Jobin Yvon Raman spectrometer (Paris, France). The Raman spectrum acquisition signal was 514 nm, laser power was 5 mW, exposure time was 2 s, scanning time was 8 s, cumulative number of repeats was three times, and the scanning range was 200–3000 cm^{-1}. Raman spectrum scanning needs two preprocessing steps: baseline correction and smoothing noise reduction. Origin Pro2021 was used for curve drawing and smoothing.

3. Results

3.1. Selection of the Best Recrystallization Antisolvent

Figure 1A shows that the taxanes in *Taxus cuspidata* were extracted with ethyl acetate. Among the eight taxanes, the highest purity was found for 10-DAT and paclitaxel (PTX), followed by the purity of 10-DAB III, the purity of cephalomannine (CEPH), docetaxel (DOT), and baccatin III (BAC III) was similar, and the purity of 7-epitaxol and DXT was the lowest. After the extraction of *Taxus cuspidata* with ethyl acetate, among the eight taxanes, the recovery rate of 10-DAB III was the highest, followed by cephalomannine (CEPH) and docetaxel (DOT), both of which were more than 80%, while the recovery rate of DXT was the lowest, being only 57.07%, which indicates that the loss of 10-DAB III was the smallest and the loss of DXT was the largest in the process of extracting *Taxus cuspidata* with ethyl acetate.

Figure 1B illustrates that the taxanes in *Taxus cuspidata* were recrystallized using methanol as the solvent and n-hexane as the antisolvent. Among the eight taxanes, the highest purity was achieved with paclitaxel (PTX) and 10-DAT, followed by cephalomannine (CEPH), and the lowest purity was achieved with 7-epitaxol (7-EPT) and docetaxel (DOT). After the recrystallization of *Taxus cuspidata* with n-hexane, among the eight taxanes, the recovery rate of 10-DAB III was the highest, and that of baccatin III (BAC III) and DXT was the lowest, being 61.71% and 55.33%, respectively. This shows that during the process of the recrystallization of taxanes from *Taxus cuspidata* with n-hexane, the loss of 10-DAB III was the smallest, while the loss of baccatin III (BAC III) and DXT was the largest.

Figure 1C shows that the taxanes in *Taxus cuspidata* were recrystallized with methanol as the solvent and petroleum ether as the antisolvent. Among the eight taxanes, the highest purity was paclitaxel (PTX) and 10-DAT, followed by cephalomannine (CEPH), and DXT achieved the lowest purity of 0.09%. After recrystallizing *Taxus cuspidata* with petroleum ether, among the eight taxanes, the recovery rate of 10-DAB III was the highest, and that of DXT was the lowest, at 43.39%. This shows that the loss of 10-DAB III was the smallest and the loss of DXT was the largest in the process of recrystallizing taxanes from *Taxus cuspidata* with petroleum ether.

Figure 1D demonstrates that the taxanes in *Taxus cuspidata* were recrystallized with methanol as the solvent and water as the antisolvent. Among the eight taxanes, the highest purity was achieved by paclitaxel (PTX) and 10-DAT, followed by docetaxel (DOT) and cephalomannine (CEPH), and DXT achieved the lowest purity of 0.10%. After the recrystallization of *Taxus cuspidata*, among the eight taxanes, the recovery rates of cephalomannine (CEPH) and paclitaxel (PTX) were the highest, while the recovery rates of baccatin III (BAC III) and DXT were the lowest, being 55.61% and 51.29%, respectively. This shows that during the recrystallization of taxanes from *Taxus cuspidata* with water, the loss of cephalomannine (CEPH) and paclitaxel (PTX) was the smallest, while the loss of baccatin III (BAC III) and DXT was the largest.

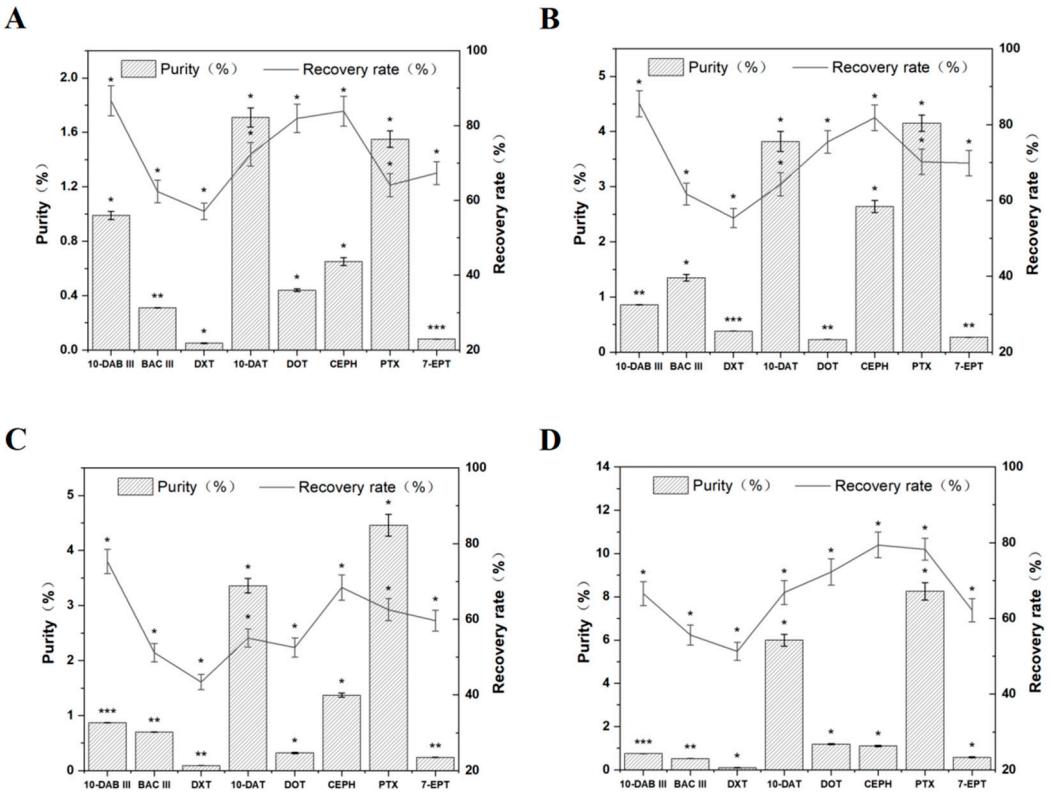

Figure 1. (**A**) Effects of ethyl acetate extraction, (**B**) n-hexane as the antisolvent for recrystallization, (**C**) petroleum ether as the antisolvent for recrystallization, and (**D**) water as the antisolvent for recrystallization on the purity and recovery of taxanes in *Taxus cuspidata* ($p < 0.05$ indicated by *, $p < 0.005$ indicated by **, and $p < 0.001$ indicated by ***).

3.2. Analysis of Taxus cuspidata before and after Recrystallization by HPLC

Figure 2A shows the HPLC diagram for eight taxane standards. Compound 1 was 10-deacetylbaccatin III (10-DAB III), compound 2 was baccatin III (BAC III), compound 3 was 7-xylogan-10-deacetyltaxol (DXT), compound 4 was 10-deacetyltaxol (10-DAT), compound 5 was docetaxel (DOT), compound 6 was cephalomannine (CEPH), compound 7 was paclitaxel (PTX), and compound 8 was 7-epitaxol (7-EPT). Figure 2B shows the HPLC chart of the crude extract of *Taxus cuspidata*, from which it can be seen that the impurities in *Taxus cuspidata* before purification accounted for a large proportion, especially the impurities with high polarity, with a peak time of 0–5 min. The purity of taxanes was very low, at only 0.20%. As can be seen from Figure 2C, the substances 1–8 in Figure 2C correspond to taxanes with numbers 1–8 in Figure 2A. *Taxus cuspidata* was purified by using water as the recrystallization antisolvent, and most of the impurities such as sugars, surfactants, and flavonoids were removed. Figure 2D was the HPLC chart of the water layer of the recrystallization product. It can be seen that there were almost no peaks at the peak positions of the eight taxanes, and there were obvious absorption peaks at the peak time of 0–5 min, indicating that some water-soluble impurities have been removed.

In summary, when water was used as the recrystallization antisolvent, the purity of taxanes in *Taxus cuspidata* was the highest. Therefore, methanol was used as the solvent and water was used as the antisolvent. Four factors, crude extraction concentration, antisolvent to solvent volume ratio, deposition temperature and deposition time, which have great influence on the crystallization effect, were selected for the single-factor experiment, and then the optimal recrystallization conditions were determined by response surface methodology.

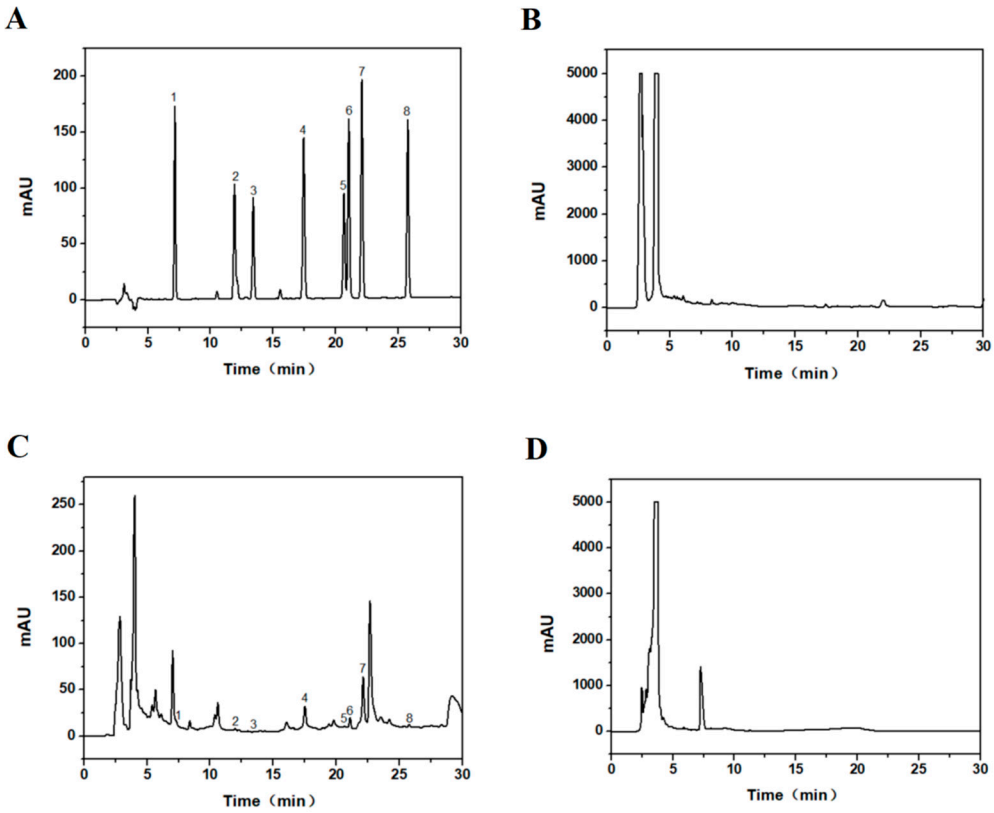

Figure 2. (**A**) HPLC detection chart of eight taxane standards (125 μg/mL), (**B**) HPLC chart of the crude *Taxus cuspidata* extract before purification, (**C**) HPLC chart after purification with water as the recrystallization antisolvent, and (**D**) HPLC chart of the recrystallized water layer.

3.3. Single-Factor Experiments

3.3.1. Crude Extraction Concentration

The crude extraction concentration was one of the main factors affecting the purity of taxanes by recrystallization. We evaluated the effect of crude extraction concentration on the purity of taxanes. As shown in Figure 3A, the purity and recovery rate of taxanes first increased and then decreased with the increase in the crude extraction concentration, reaching the maximum when the crude extraction concentration was 500 mg/mL. This phenomenon may be due to the fact that *Taxus cuspidata* contains many components, among which the solubility of taxanes in methanol is better than that of other components. Therefore, when the crude extraction concentration increases, the concentration of taxanes in the solution increases by more than that of other components. When other factors remain the same, the equilibrium concentration of each component in the mixed system remains the same, and the concentration of taxanes increases greatly, causing the increase in supersaturation to be more than that of other components. An increase in supersaturation can lead to a decrease in the Gibbs free energy [47], and the decrease in the Gibbs free energy of taxanes in the mixed system is larger than that of other components, so that the probability of the taxane nucleation is higher than that of other components. When the crude extraction concentration exceeds 500 mg/mL, other impurity components gradually precipitate, resulting in a decrease in the purity and recovery rate of taxanes. Therefore, in this study, the optimized range of crude extraction concentration was 400–600 mg/mL.

3.3.2. Antisolvent to Solvent Volume Ratio

The antisolvent to solvent volume ratio was one of the main factors affecting the purity of taxanes following recrystallization. We evaluated the effect of the antisolvent to solvent volume ratio on the purity of taxanes. As shown in Figure 3B, the purity and recovery rate of taxanes first increased and then tended to be flat with an increase in the antisolvent to solvent volume ratio, and reached a maximum when the volume of the antisolvent was 25 times that of the solvent. This may be because when the volume of antisolvent was between 5 and 25 times that of the solvent, the actual and equilibrium concentrations of taxanes in the mixed system decreased with the increase in the antisolvent in the mixed system. However, the supersaturation of components in the mixed system increased because the decreasing rate of the equilibrium concentration was greater than the actual concentration. Therefore, the purity of the taxanes increases with the increase in volume ratio during the process of increasing the volume of antisolvent from 5 to 25 times that of the solvent volume. However, when the volume of antisolvent was 25 times that of the solvent volume, the actual concentration of taxanes in the mixed system was already very small. When the volume ratio of the antisolvent continued to increase, the supersaturation rate of components in the *Taxus cuspidata* extract gradually decreased or no longer increased [48]. At this time, the crystallization rate of various components in the *Taxus cuspidata* extract was almost constant, which led to the volume of antisolvent increasing from 25 to 20 times that of the solvent volume, and the purity and recovery rate of the taxanes tended to be flat. Therefore, in this study, the antisolvent to solvent volume ratio was further optimized to 20–30 times.

3.3.3. Deposition Temperature

The deposition temperature was one of the main factors affecting the purity of the taxanes by recrystallization. We evaluated the effect of the deposition temperature on the purity of taxanes. As shown in Figure 3C, when the deposition temperature increased from 20 °C to 45 °C, the purity and recovery rate of the taxanes decreased gradually with the increase in deposition temperature. The reason for this phenomenon may be that the equilibrium concentration of various components in the mixed system of *Taxus cuspidata* is greatly affected by temperature. With the increase in temperature, the equilibrium concentration of taxanes and other components in the mixed system of *Taxus cuspidata* increased, and the supersaturation decreased. However, the supersaturation of taxanes was lower than that of the other components, which caused the crystallization rate of taxanes to be lower than that of the other components, with the other factors being unchanged. Therefore, when the temperature was higher than 30 °C, the purity and recovery of the taxanes decreased gradually. Moreover, when the temperature was low, the relative solubility of the substance was low, and it became easier for the taxanes to reach saturation and precipitate in the solution [49]. When the temperature was raised, the solubility of the taxanes also improved, which is not conducive to the precipitation of taxanes, resulting in a decrease in the purity and recovery rate of taxanes. Therefore, only when the temperature is appropriate can a higher purity of taxanes be obtained. For this reason, in this study, the further optimization range of the deposition temperature was 20–30 °C.

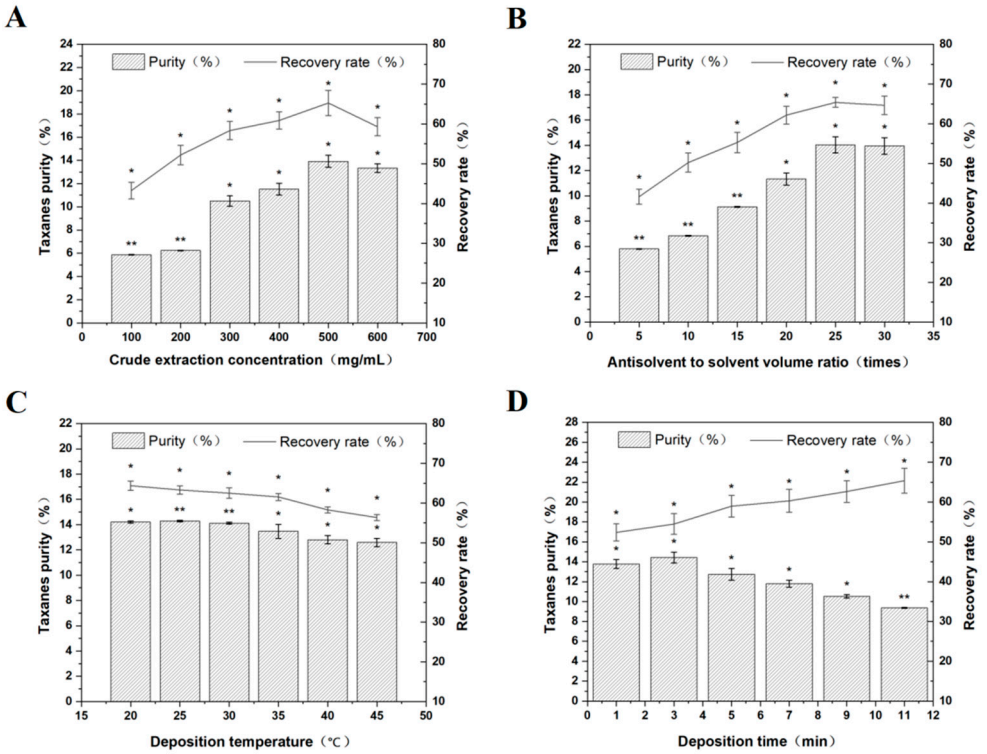

Figure 3. Effects of (**A**) the crude extraction concentration, (**B**) antisolvent to solvent volume ratio, (**C**) deposition temperature, and (**D**) deposition time on the purity of eight taxanes in *Taxus cuspidata* ($p < 0.05$ indicated by *, $p < 0.005$ indicated by **).

3.3.4. Deposition Time

The deposition time was one of the main factors affecting the purity of taxanes by recrystallization. We evaluated the effect of deposition time on the purity of taxanes. As shown in Figure 3D, it can be seen from the obtained results that the purity of taxanes first increased and then decreased with the increase in deposition time, and the recovery rate of the taxanes increased with the increase in deposition time. The reason for this trend may be that the supersaturation of taxanes in the mixed system was higher than that of other components, which caused its nucleation rate to be higher than that of other components. The solubility of taxanes in water is very low, and when the taxanes are completely dissolved in methanol, the taxanes precipitate rapidly after adding deionized water. When the deposition time reached 3 min, almost all of the taxanes supersaturated in *Taxus cuspidata* precipitated, and the amount of taxanes precipitated reached its maximum. However, when the deposition time exceeded 3 min, a large number of other impurities were precipitated, resulting in the decreasing purity of taxanes. In addition, the precipitation of taxanes was more complete with the increase in time, so the recovery rate of taxanes gradually increased with the increase in the deposition time. Taking the purity as the reference value, the further optimized range of deposition time in this study was 1–3 min.

3.4. Construction of the RSM Model and the Optimization of Conditions

The response surface data analysis software Design Expert 12 was used to analyze the test data shown in Table 1, and the quadratic polynomial regression equation of the relationship between the taxanes purity (Y), crude extraction concentration (X_1), antisolvent to solvent volume ratio (X_2), deposition temperature (X_3), and deposition time (X_4) was obtained:

$$Y = 20.24 + 1.67X_1 + 3.18X_2 + 1.05X_3 - 2.97X_4 + 2.57X_1X_2 - 1.13X_1X_3 + 0.081X_1X_4$$

$$- 1.62X_2X_3 - 1.19X_2X_4 + 0.27X_3X_4 - 2.60{X_1}^2 - 3.47{X_2}^2 - 0.92{X_3}^2 - 2.21{X_4}^2$$

The analysis of variance is shown in Table 2. As can be seen from Table 2, the F value of the model was 37.52, $p < 0.0001$, which indicates that the model was highly significant, and the misfitting term was $p = 0.4353 > 0.05$, which indicates that the regression equation was not yet fitted, that is to say, there was no significant influence of the other factors except for those considered in this experiment, and the regression model fit the real response value well. The model-adjusted R^2 was 0.9481 and the predicted R^2 was 0.8763, since the adjusted R^2 value was very high and close to the predicted R^2 value, which indicates that the regression equation can fully explain the technological process. The model can be used to analyze and predict the optimal conditions of the interaction of four single factors during recrystallization, in terms of the effect on the purity of taxanes in *Taxus cuspidata*.

Table 1. The experimental design and results of the Box–Behnken design (BBD).

Run	X_1	X_2	X_3	X_4	Taxanes Purity (%)
1	400.00	25.00	25.00	5.00	10.6358
2	400.00	20.00	25.00	3.00	12.5983
3	400.00	25.00	25.00	1.00	17.3129
4	500.00	30.00	30.00	3.00	19.1577
5	600.00	25.00	30.00	3.00	18.3369
6	500.00	30.00	25.00	5.00	13.1014
7	500.00	25.00	25.00	3.00	20.3471
8	500.00	25.00	30.00	1.00	21.2453
9	500.00	20.00	25.00	1.00	13.3078
10	500.00	25.00	25.00	3.00	19.1931
11	600.00	20.00	25.00	3.00	10.4839
12	500.00	25.00	20.00	5.00	12.5033
13	500.00	25.00	25.00	3.00	20.6922
14	500.00	25.00	20.00	1.00	18.7964
15	500.00	20.00	25.00	5.00	10.1201
16	600.00	25.00	25.00	5.00	13.985
17	500.00	20.00	30.00	3.00	14.0391
18	500.00	30.00	20.00	3.00	21.1741
19	400.00	25.00	30.00	3.00	16.7901
20	500.00	20.00	20.00	3.00	9.5607
21	400.00	25.00	20.00	3.00	12.4958
22	500.00	25.00	25.00	3.00	19.6704
23	500.00	25.00	25.00	3.00	21.2981
24	600.00	30.00	25.00	3.00	20.9644
25	600.00	25.00	25.00	1.00	20.3397
26	500.00	25.00	30.00	5.00	16.0481
27	400.00	30.00	25.00	3.00	12.7904
28	600.00	25.00	20.00	3.00	18.5439
29	500.00	30.00	25.00	1.00	21.0477

The crude extraction concentration, antisolvent to solvent volume ratio, and deposition time had extremely significant effects on the purity of taxanes in *Taxus cuspidata*, and the deposition temperature had more significant effects. However, the rates of contribution of these four factors to the purity of taxanes were different, in the order $X_2 > X_4 > X_1 > X_3$. The interaction between the crude extraction concentration and antisolvent to solvent volume ratio was extremely significant; that between the antisolvent to solvent volume ratio and deposition temperature was more significant; that between the crude extraction concentration and deposition temperature, antisolvent to solvent volume ratio and deposition time was significant; and that between the crude extraction concentration and deposition time, deposition temperature and deposition time was not significant. The square terms of the crude extraction concentration, antisolvent to solvent volume ratio, and deposition time were extremely significant, and the square term of the deposition temperature was significant.

Table 2. The ANOVA of the regression model.

Source of Variation	Sum of Squares	Degree of Freedom	Mean Square	F-Value	*p*-Value	Significance
Model	436.06	14	31.15	37.52	<0.0001	***
X_1	33.44	1	33.44	40.28	<0.0001	***
X_2	121.13	1	121.13	145.91	<0.0001	***
X_3	13.11	1	13.11	15.79	0.0014	**
X_4	105.95	1	105.95	127.62	<0.0001	***
X_1X_2	26.46	1	26.46	31.88	<0.0001	***
X_1X_3	5.07	1	5.07	6.10	0.0270	*
X_1X_4	0.026	1	0.026	0.031	0.8621	
X_2X_3	10.55	1	10.55	12.70	0.0031	**
X_2X_4	5.66	1	5.66	6.82	0.0205	*
X_3X_4	0.30	1	0.30	0.36	0.5572	
${X_1}^2$	43.89	1	43.89	52.87	<0.0001	***
${X_2}^2$	78.00	1	78.00	93.96	<0.0001	***
${X_3}^2$	5.54	1	5.54	6.68	0.0216	*
${X_4}^2$	31.55	1	31.55	38.00	<0.0001	***
Residual	11.62	14	0.83			
Lack of fit	8.87	10	0.89	1.29	0.4353	
Pure error	2.76	4	0.69			
Total	447.68	28				

Note: $p \leq 0.0001$ is extremely significant, as indicated by ***; $p \leq 0.01$ is more significant, indicated by **; and $p \leq 0.05$ is significant, as indicated by *.

As shown in Figure 4, the interaction between the crude extraction concentration (X_1) and antisolvent to solvent volume ratio (X_2) was the strongest; the interaction between the antisolvent to solvent volume ratio (X_2) and deposition temperature (X_3) was more significant; and the interactions between the crude extraction concentration (X_1) and deposition temperature (X_3), and between the antisolvent to solvent volume ratio (X_2) and deposition time (X_4) were the weakest. With the increase in the crude extraction concentration (X_1), the purity of the taxanes first increased and then decreased; with the increase in the antisolvent to solvent volume ratio (X_2), the purity of the taxanes increased gradually; and with the increase in deposition time (X_4), the purity of the taxanes first increased and then decreased, which was consistent with the single-factor results. Based on the multiple quadratic regression equation, we calculated the best experimental conditions in terms of the crude extraction concentration, antisolvent to solvent volume ratio, deposition temperature, and deposition time, which were as follows: the crude extraction concentration was 555.28 mg/mL, the antisolvent to solvent volume ratio was 28.16 times, the deposition temperature was 22.91 °C, the deposition time was 1.76 min, and the purity of the taxanes reached the maximum value of 23.482%. Under these conditions, the actual purity of the taxanes was 23.238%, which was very close to the predicted purity of 23.482%. All of the data demonstrate that the model is feasible for parameter optimization in the process of purifying taxanes.

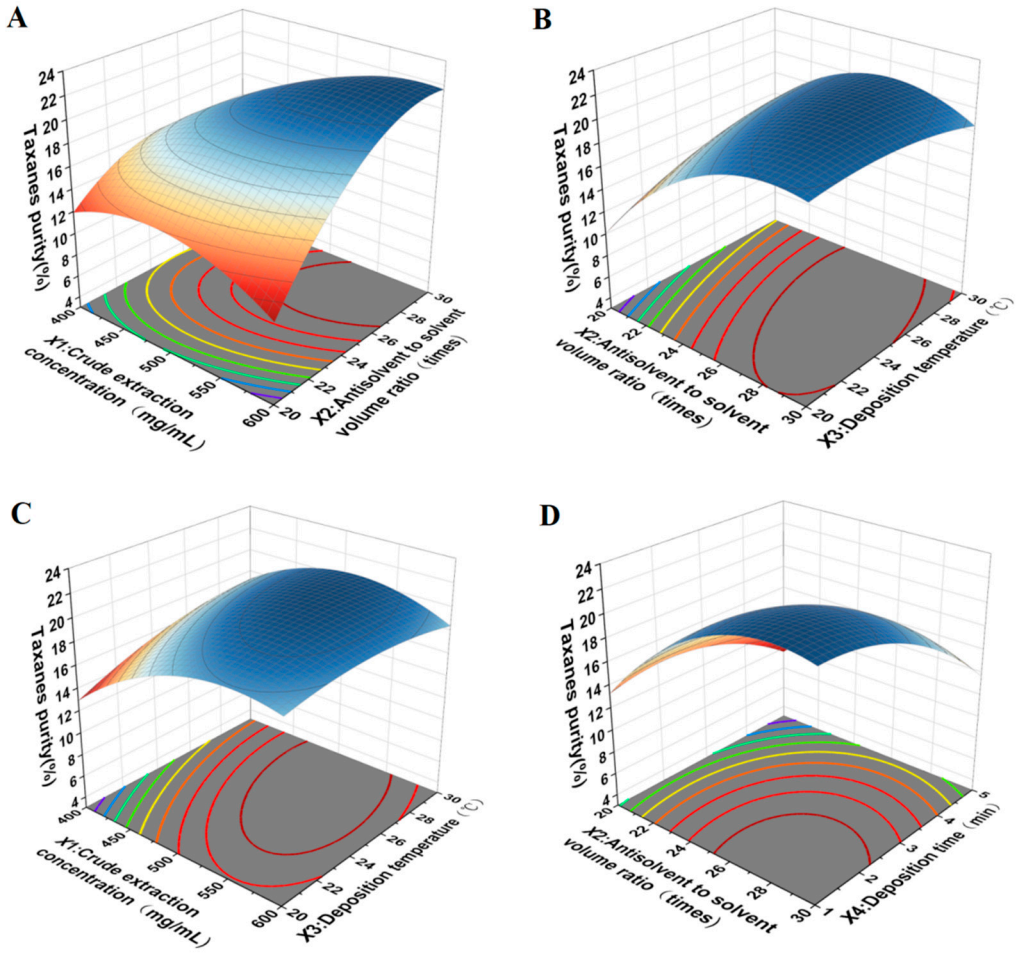

Figure 4. Interaction diagram of various factors: (**A**) crude extraction concentration and antisolvent to solvent volume ratio; (**B**) antisolvent to solvent volume ratio and deposition temperature; (**C**) crude extraction concentration and deposition temperature; and (**D**) antisolvent to solvent volume ratio and deposition time.

3.5. SEM Analysis of Taxus cuspidata before and after Recrystallization

Figure 5 illustrates that the particle size distribution of the crude *Taxus cuspidata* was nonuniform and the particle shape of *Taxus cuspidata* was irregular (Figure 5A,B), with values in the range of 10–550 μm (the particle size distribution is shown in Figure 5E). However, the particle size distribution and particle morphology of *Taxus cuspidata* products prepared by antisolvent recrystallization were obviously improved, the particle morphology was generally bar-shaped (Figure 5C,D), and the particle size was obviously much smaller than that of the crude *Taxus cuspidata* products, most of which were distributed around 300 nm (the particle size distribution diagram is shown in Figure 5F). The results showed that during recrystallization, not only was the purity of the effective components in *Taxus cuspidata* significantly increased, but the particle size of *Taxus cuspidata* could also be effectively reduced, and the morphology of particles could be well-controlled.

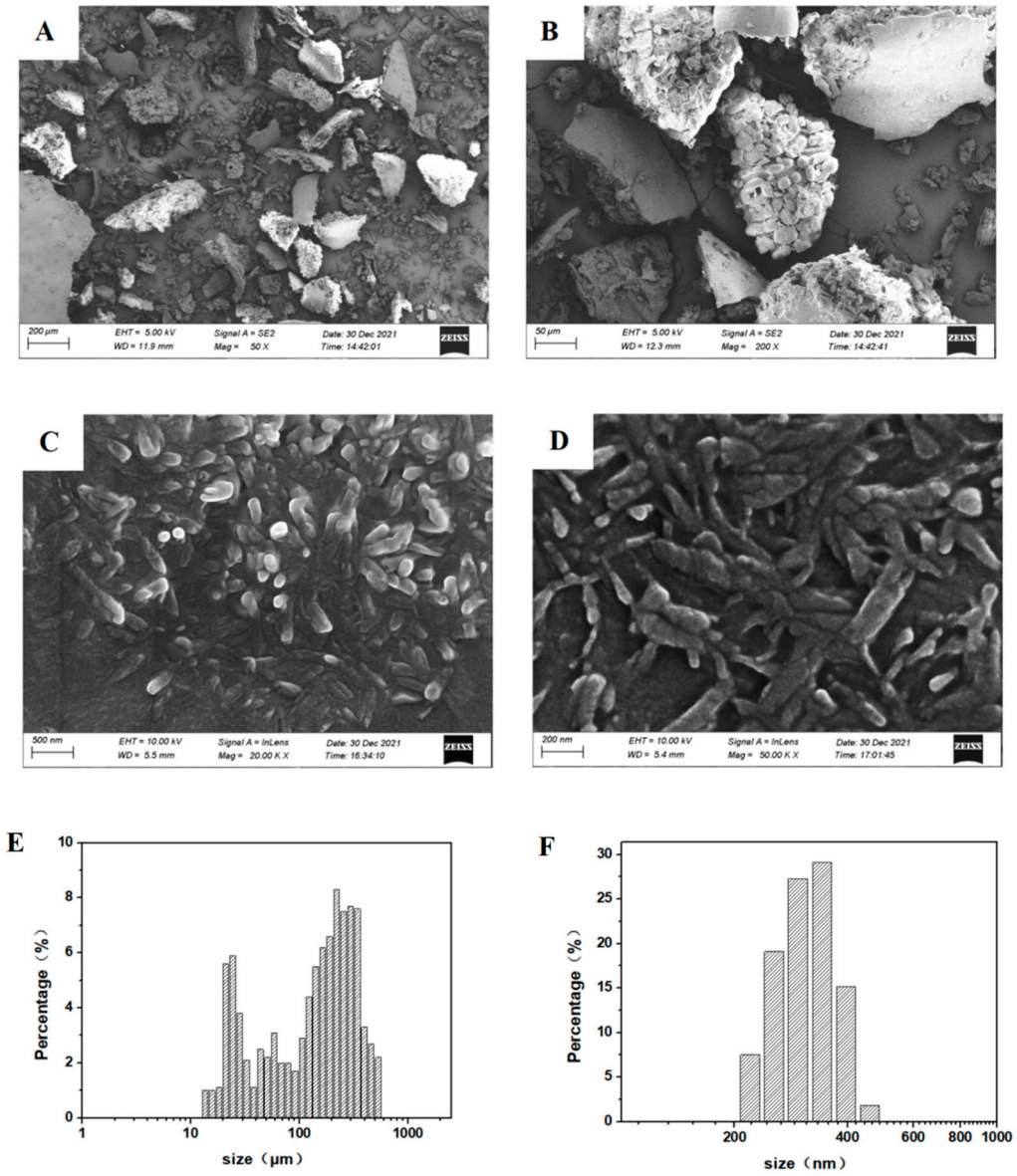

Figure 5. SEM detection chart and particle size distribution of the (**A**,**B**) crude *Taxus cuspidata* and (**C**,**D**) the recrystallized product of *Taxus cuspidata*; (**E**) particle size distribution diagram of the crude *Taxus cuspidata*; (**F**) grain size distribution diagram of the recrystallized product.

3.6. XRD and Raman Spectroscopic Analysis of the Crude and Recrystallization Products

In this experiment, the crystal forms of the crude and recrystallized products of *Taxus cuspidata* were detected and compared. Figure 6A shows the XRD detection chart of the crude and recrystallized products of *Taxus cuspidata*. There was no obvious diffraction peak in the XRD spectrum of the crude *Taxus cuspidata*, which may be due to the amorphous state of the crude *Taxus cuspidata* complex components (Figure 6A(a)). There was no obvious diffraction peak in the XRD spectrum of the recrystallized product of *Taxus cuspidata* (Figure 6A(b)), which indicates that the amorphous state of the crude *Taxus cuspidata* did not change in the process of antisolvent recrystallization, and that it always remained amorphous.

In this experiment, the crude and recrystallized products of *Taxus cuspidata* were detected and compared by their Raman spectra. Figure 6B shows the Raman spectra of the crude and recrystallized products of *Taxus cuspidata*, from which it can be seen that there was no obvious difference between the Raman spectra of the crude *Taxus cuspidata* and recrystallized product. Characteristic Raman peaks concentrated in the range of

620–200 cm^{-1} may be related to the skeleton deformation and vibration of *Taxus cuspidata*. The characteristic Raman peak around 1085 cm^{-1} may be related to the stretching vibration of the aromatic C–C–O ring. The characteristic Raman peak around 391 cm^{-1} may be related to phenolic O–H bending vibration and CH_3 bending vibration. The characteristic Raman peak around 593 cm^{-1} may be related to the symmetric stretching vibration of the aromatic ring. Characteristic Raman peaks concentrated in the range of 1600–1000 cm^{-1} were mainly related to more oil and wax in *Taxus cuspidata*. The characteristic Raman peaks concentrated in the range of 3000–2200 cm^{-1} may be related to the stretching vibration of aliphatic C–H and CH_2 in *Taxus cuspidata*.

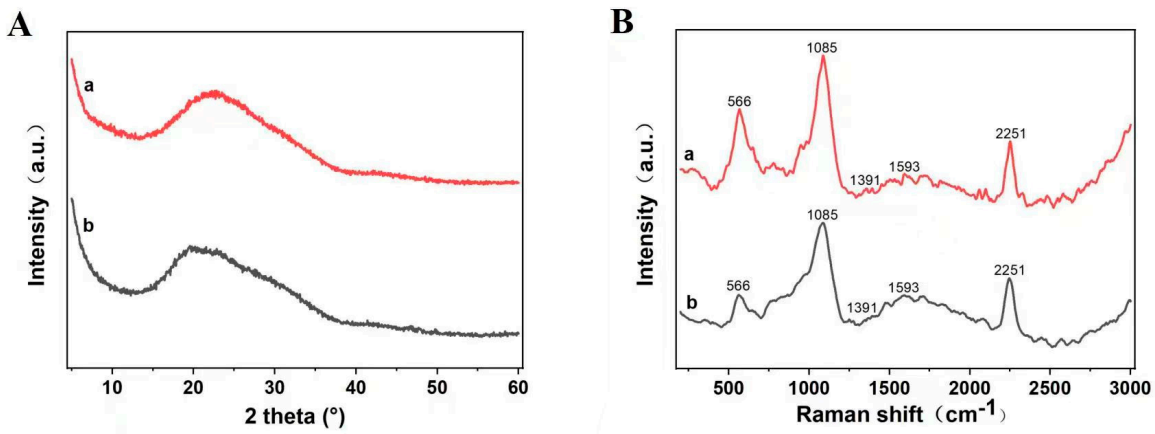

Figure 6. (**A**) XRD pattern and (**B**) Raman spectrum of *Taxus cuspidata*. (a) crude *Taxus cuspidata*, (b) recrystallization product.

In recent years, some scholars have conducted much research on the separation and purification of taxanes. Kim et al. developed an ultrasonic-assisted micellar extraction process that was used to efficiently purify the anticancer substance paclitaxel from the plant cell *Taxus chinensis*. The problem of many extraction steps and a long phase separation time in the traditional micellar process could be dramatically improved. The highest paclitaxel yield was obtained at 180 W of ultrasonic power and 1.5 h of ultrasonic irradiation time, which was 24.7% higher than that of the traditional method, and the purity of the initial paclitaxel (6.81%) increased to 22.0% [50]. Min et al. showed that the precipitation efficiency of paclitaxel from *Taxus chinensis* was remarkably improved through negative pressure cavitation fractional precipitation. When paclitaxel was precipitated under a negative pressure of −200 mmHg, almost all of the paclitaxel (<97%) could be recovered in a short operation time (1 min). In addition, the application of negative pressure reduced the size of the precipitate by 3.3 times and increased the diffusion coefficient of paclitaxel by 4.4 times [51]. Kang et al. developed an improved acetone–water fractional precipitation process for paclitaxel using ultrasonic cavitation bubbles and gas bubbles. Compared with the conventional method, the time required for precipitation was reduced by 20–25 times. In addition, the particle size of paclitaxel decreased by 3.5–5.5 times and the diffusion coefficient of paclitaxel increased by 3.5–6.7 times [52]. Park et al. investigated the effect of tar compounds on the purification efficiency of paclitaxel from *Taxus chinensis* and evaluated the adsorbent for their removal. The tar compounds had an adverse effect on the purification process in increasing order: 1-methylnaphthalene, o-xylene < acenaphthene < 2-picoline < 2,5-xylenol. As a result of adsorbent treatment, the macroporous adsorption resin (DIAION HP20) gave the highest yield (97.8%) and purity (44.7%) of paclitaxel [53].

In this study, although the purity of the taxanes in *Taxus cuspidata* purified by the antisolvent recrystallization method was 23.238%, the purity of the taxanes before purification was only 0.20% due to the complex components of *Taxus cuspidata*, and the structure of the product was not damaged during recrystallization. Therefore, the antisolvent recrystallization method is suitable for the preliminary purification of taxanes.

4. Conclusions

An efficient preliminary purification method of taxanes from *Taxus cuspidata* was established, and the antisolvent recrystallization purification process of taxanes was optimized by response surface methodology. When the crude extraction concentration was 555.28 mg/mL, the antisolvent to solvent volume ratio was 28.16 times, the deposition temperature was 22.91 °C, and the deposition time was 1.76 min, the purity of the taxanes was at its highest. The SEM results showed that recrystallization could effectively reduce the particle size of the crude *Taxus cuspidata* and control the particle morphology. The XRD and Raman spectrum experiments showed that the amorphous state of the crude *Taxus cuspidata* did not change during the antisolvent recrystallization process and always remained amorphous. After the purification of taxanes from *Taxus cuspidata* by recrystallization, the purity of the taxanes increased from the original 0.20% to 23.238%.

Author Contributions: Conceptualization, Y.Z., W.L. and Y.T.; Methodology, Y.Z. and Z.Z.; Software, Y.Z.; Validation, Y.Z., Z.Z. and H.M.; Formal analysis, Y.Z.; Investigation, Y.Z., Z.Z., W.L. and Y.T.; Resources, Y.Z.; Data curation, Y.Z.; Writing—original draft preparation, Y.Z.; Writing—review and editing, S.W.; Visualization, S.W.; Supervision, S.W.; Funding acquisition, S.W. All authors have read and agreed to the published version of the manuscript.

Funding: This research was funded by "The 13th Five Year Plan" for Nation Science and Technology in Rural Area (No. 3G016W112418); Jilin Province Science and Technology Development Key Program (No. 20180201009NY); Changchun City Science and Technology Development Program (No. NK15SS22); and Key Laboratory of Ministry of Education (No. K201101).

Institutional Review Board Statement: Not applicable.

Informed Consent Statement: Not applicable.

Data Availability Statement: The data shown in this study are contained within the article.

Acknowledgments: The authors would like to extend their appreciation to the development plan project during "The 13th Five Year Plan" for Nation Science and Technology in Rural Area (No. 3G016W112418), Jilin Province Science and Technology Development Key Program (No. 20180201009NY); Changchun City Science and Technology Development Program (No. NK15SS22); and Key Laboratory of Ministry of Education (No. K201101).

Conflicts of Interest: The authors declare no conflict of interest.

References

1. Miller, R.W.; Powell, R.G.; Smith, C.R.; Arnold, E.; Clardy, J. Antileukemic alkaloids from *Taxus* wallichiana zucc. *J. Org. Chem.* **1981**, *46*, 1469–1474. [CrossRef]
2. Lange, B.M.; Conner, C.F. Taxanes and taxoids of the genus *Taxus*–A comprehensive inventory of chemical diversity. *Phytochemistry* **2021**, *190*, 112829. [CrossRef] [PubMed]
3. Wang, T.; Li, L.; Zhuang, W.; Zhang, F.; Wang, Z. Recent research progress in taxol biosynthetic pathway and acylation reactions mediated by *Taxus* acyltransferases. *Molecules* **2021**, *26*, 2855. [CrossRef] [PubMed]
4. Fett-Neto, A.G.; Dicosmo, F.; Reynolds, W.F.; Sakata, K. Cell culture of *taxus* as a source of the antineoplastic drug taxol and related taxanes. *Bio/Technology* **1992**, *10*, 1572–1575. [CrossRef] [PubMed]
5. Moore, A.L.; Butcher, M. Functional specialization in the forelimbs of two digging mammals: The american badger (taxidea *taxus*) and groundhog (marmota monax). *FASEB J.* **2011**, *25*, 3515–3524. [CrossRef]
6. Liu, D.; Guo, Z.; Cui, X.; Fan, C. Comparison of five associations of *Taxus cuspidata* and their species diversity. *Biodivers. Sci.* **2020**, *28*, 94–105. [CrossRef]
7. Xiang, Y.; Liu, J.; Liu, D.; Lu, A.; Wu, W. Identification of *Taxus cuspidata* Sieb.et Zucc endophytic fungi-new recorded-genus-species of China and the metabolite. *J. For. Res.* **2004**, *15*, 61–66. [CrossRef]
8. Xiang, Y.; Lu, A.; Wu, W. Identification of *Taxus cuspidata* sieb. et Zucc. endophytic fungi-new species, species known and their metabolite. *J. For. Res.* **2003**, *14*, 290–294. [CrossRef]
9. Cheng, Q.; Oritani, T.; Horiguchi, T. Four Novel Taxane Diterpenoids from the Needles of Japanese Yew, *Taxus cuspidata*. *Biosci. Biotechnol. Biochem.* **1999**, *64*, 894–898. [CrossRef]
10. Jiang, P.; Zhao, Y.; Xiong, J.; Wang, F.; Yu, X. Extraction, Purification, and Biological Activities of Flavonoids from Branches and Leaves of *Taxus cuspidata* S. et Z. *Bioresources* **2021**, *16*, 2655–2682. [CrossRef]

11. Zhang, S.; Lu, X.; Zheng, T.; Guo, X.; Tang, Z. Investigation of bioactivities of *Taxus chinensis*, *Taxus cuspidata*, and *Taxus* × *media* by gas chromatography-mass spectrometry. *Open Life Sci.* **2021**, *16*, 287–296. [CrossRef] [PubMed]
12. Tong, X.; Fang, W.; Zhou, J.; He, C.; Chen, W.; Fang, Q. Three New Taxane Diterpenoids from Needles and Stems of *Taxus cuspidata*. *J. Nat. Prod.* **2004**, *58*, 233–238. [CrossRef]
13. Kawamura, F.; Kikuchi, Y.; Ohira, T.; Yastagai, M. Phenolic constituents of *Taxus cuspidata* I: Lignans from the roots. *J. Wood Sci.* **2000**, *46*, 167–171. [CrossRef]
14. Ni, Z.; Wu, Y.; Dong, M.; Zhang, M.; Wang, Y.; Françoise, S.; Huo, C.; Shi, Q.; Gu, Y.; Hiromasa, K.; et al. Diabietane ether, a new dimeric abietane with an ether linkage from *Taxus cuspidata* needles. *Z. Naturforsch. B.* **2011**, *66*, 1083–1086. [CrossRef]
15. Li, X.; Yu, X.; Guo, W.; Li, Y.; Liu, X.; Wang, N.; Liu, B. Genomic diversity within *Taxus cuspidata* var. nana revealed by random amplified polymorphic DNA markers. *Russ. J. Plant Physiol.* **2006**, *53*, 684–688. [CrossRef]
16. Lenka, S.K.; Nims, N.E.; Vongpaseuth, K.; Boshar, R.A.; Roberts, S.C.; Walker, E.L. Jasmonate-responsive expression of paclitaxel biosynthesis genes in *Taxus cuspidata* cultured cells is negatively regulated by the bHLH transcription factors TcJAMYC1, TcJAMYC2, and TcJAMYC4. *Front. Plant Sci.* **2015**, *6*, 115–128. [CrossRef]
17. Kishiko, O.; Sanro, T.; Masaya, S. Electron Microscopic Observation of Plastid Containing Taxol-like Substances in Callus Cells of *Taxus cuspidata* var. Nana. *Pak. J. Biol. Sci.* **2004**, *7*, 1028–1034. [CrossRef]
18. Liu, T.; Zhou, Z. Characteristics of natural Japanese yew population in Muling Nature Reserve of Heilongjiang Province, China. *J. For. Res.* **2006**, *17*, 132–134. [CrossRef]
19. Shi, Q.; Oritani, T.; Sugiyama, T. Three novel bicyclic taxane diterpenoids with verticillene skeleton from the needles of Chinese yew, *Taxus chinensis* var. Mairei. *Planta Med.* **1999**, *62*, 1114–1118. [CrossRef]
20. Yao, X.; Da, B.; Chen, J.; Li, X.; Tang, B. Tissue culture and analysis on taxane diterpenoids in callus of *Taxus chinensis* var. Mairei, Chin. Tradit. *Herb. Drugs.* **2014**, *45*, 2696–2702. [CrossRef]
21. Fan, X.; Wang, L.; Chang, Y.; An, J.; Fu, Y. Application of green and recyclable menthol-based hydrophobic deep eutectic solvents aqueous for the extraction of main taxanes from *Taxus chinensis* needles. *J. Mol. Liq.* **2020**, *326*, 114–122. [CrossRef]
22. Yu, S.; Zhang, M.; Wang, Y.; Huo, C.; Shi, Q. A New Taxane from the Hard Wood of *Taxus cuspidata*. *Z. Naturforsch. B.* **2010**, *65*, 635–638. [CrossRef]
23. Zhang, J.; Duan, J.; Liang, Z.; Zhang, W.; Zhang, L.; Huo, Y.; Zhang, Y. Separation and identification of Taxol in the crude extracts of *Taxus cuspidata* and its callus culture with HPLC-ESI-MS/MS. *Acta Pharmacol. Sin.* **2008**, *41*, 863–866. [CrossRef]
24. Shinjiro, Y.; Yuka, S.; Takato, K.; Shuhei, H.; Hitoshi, M. Enhanced productivity of paclitaxel and related taxanes in plant cell culture including aliphatic ionic liquids. *Solvent Extr. Res. Dev. Jpn.* **2018**, *25*, 125–130. [CrossRef]
25. Jerzy, K.; Atwal, A.S.; Subramaniam, M. Determination of Formaldehyde in Fresh and Retail Milk by Liquid Column Chromatography. *J. AOAC Int.* **1993**, *76*, 1010–1013. [CrossRef]
26. Rokosik, E.; Dwiecki, K.; Rudzińska, M.; Siger, A.; Polewski, K. Column chromatography as a method for minor components removal from rapeseed oil. *Grasas Aceites.* **2019**, *70*, 9182. [CrossRef]
27. Wang, L.; Huang, X.; Jing, H.; Ye, X.; Jiang, C.; Shao, J.; Ma, C.; Wang, H. Separation of epigallocatechin gallate and epicatechin gallate from tea polyphenols by macroporous resin and crystallization. *Anal. Methods.* **2021**, *13*, 832–842. [CrossRef]
28. Ke, C.; Ren, Y.; Gao, P.; Han, J.; Yang, X. Separation and purification of pyrroloquinoline quinone from fermentation broth by pretreatment coupled with macroporous resin adsorption. *Sep. Purif. Technol.* **2021**, *257*, 117962. [CrossRef]
29. Lee, C.G.; Kim, J.H. Improved fractional precipitation method for purification of paclitaxel. *Process Biochem.* **2014**, *49*, 1370–1376. [CrossRef]
30. Watchueng, J.; Kamnaing, P.; Gao, J.M.; Kiyota, T.; Yeboah, F.; Konishi, Y. Efficient purification of paclitaxel from yews using high-performance displacement chromatography technique. *J. Chromatogr. A.* **2011**, *1218*, 2929–2935. [CrossRef]
31. Piletska, E.; Magumba, K.; Joseph, L.; Cruz, A.G.; Norman, R.; Singh, R.; Tabasso, A.F.S.; Jones, D.J.L.; Macip, S.; Piletsky, S. Molecular imprinting as a tool for determining molecular markers: A lung cancer case. *RSC Adv.* **2022**, *12*, 17747–17754. [CrossRef] [PubMed]
32. Saeid, A.; Eun, J.B.; Sagor, M.S.A.; Rahman, A.; Akter, M.S.; Ahmed, M. Effects of Extraction and Purification Methods on Degradation Kinetics and Stability of Lycopene from Watermelon under Storage Conditions. *J. Food Sci.* **2016**, *81*, 2630–2638. [CrossRef] [PubMed]
33. Lubaina, A.S.; Renjith, P.R.; Roshni, A.S.; Thompson, J. Identification and Quantification of Polyphenols from Pineapple Peel by High Performance Liquid Chromatography Analysis. *Adv. Zool. Bot.* **2020**, *8*, 431–438. [CrossRef]
34. Sun, Y.; Wang, Y.; Luo, S. Preparative separation and enrichment of four taxoids from *Taxus chinensis* needles extracts by macroporous resin column chromatography. *J. Sep. Sci.* **2009**, *32*, 1284–1293. [CrossRef]
35. Luebbert, C.; Sadowski, G. Moisture-induced phase separation and recrystallization in amorphous solid dispersions. *Int. J. Pharm.* **2017**, *532*, 635–646. [CrossRef]
36. Karmwar, P.; Graeser, K.; Gordon, K.C.; Strachan, C.J.; Rades, T. Investigation of properties and recrystallisation behaviour of amorphous indomethacin samples prepared by different methods. *Int. J. Pharm.* **2011**, *417*, 94–100. [CrossRef] [PubMed]
37. Punochová, K.; Vukosavljevic, B.; Jaroslav, H.; Beránek, J.; Frantiek, T. Non-invasive insight into the release mechanisms of a poorly soluble drug from amorphous solid dispersions by confocal Raman microscopy. *Eur. J. Pharm. Biopharm.* **2016**, *101*, 119–125. [CrossRef] [PubMed]

38. Yadava, U.; Gupta, H.; Roychoudhury, M. Stabilization of Microtubules by Taxane Diterpenoids: Insight from Docking and MD simulations. *J. Biol. Phys.* **2015**, *41*, 117–133. [CrossRef]
39. Wang, L.; Wu, B.; Deng, W.; Liu, Y. Optimization of Ellagic Acid Purification from Pomegranate Husk by Antisolvent Recrystallization. *Chem. Eng. Technol.* **2018**, *41*, 1181–1198. [CrossRef]
40. Zhao, X.; Wu, M.; Feng, Z.; Wang, L.; Huang, Y. Purification of *Ginkgo biloba* Extract by Antisolvent Recrystallization. *Chem. Eng. Technol.* **2016**, *39*, 1301–1308. [CrossRef]
41. Tarbe, M.; Pomyers, H.D.; Mugnier, L.; Bertin, D.; Mabrouk, K. Gram-scale purification of aconitine and identification of lappaconitine in Aconitum karacolicum. *Fitoterapia* **2017**, *120*, 85–92. [CrossRef] [PubMed]
42. Alexander, W.; Samuel, A.O.; Felix, A.; Kwbena, D.; Salifu, S.L. Response surface methodology as a tool for optimization of the extraction of bioactive compounds from plant sources. *J. Sci. Food Agric.* **2022**. [CrossRef]
43. Wu, Y.; Wang, X.; Xue, J.; Fan, E. Plant Phenolics Extraction from Flos Chrysanthemi: Response Surface Methodology Based Optimization and the Correlation Between Extracts and Free Radical Scavenging Activity. *J. Food Sci.* **2017**, *82*, 2726–2733. [CrossRef] [PubMed]
44. Tian, G.; Yin, X.; Peng, X.; Li, C.; Wang, T.; Feng, J.; Ju, R. Response Surface Methodology Optimized Pilot Plant Extraction Process of 1-Deoxynojirimycin from Mulberry Leaves. *J. Biobased Mater. Bioenergy* **2019**, *13*, 207–213. [CrossRef]
45. Kwak, H.J.; Park, S.J.; Kim, Y.N.; Yoo, G.; Jeong, E.J.; Kim, S.H. Optimization of extraction conditions for enhancing estrogenic activity of Rheum undulatum Linné using response surface methodology. *Sep. Sci. Technol.* **2020**, *55*, 2080–2089. [CrossRef]
46. Zhang, Y.; Zhao, Z.; Meng, H.; Wang, S. Ultrasonic Extraction and Separation of Taxanes from *Taxus cuspidata* Optimized by Response Surface Methodology. *Separations* **2022**, *9*, 193. [CrossRef]
47. Yazdani, F.; Edrissi, M. Effect of pressure on the size of magnetite nanoparticles in the coprecipitation synthesis. *Mater. Sci. Eng.* **2010**, *171*, 86–89. [CrossRef]
48. Zhu, Y.; Demilie, P.; Davoine, P.; Paule, M. Application of density meter in the supersaturation determination of the two-component equilibrium systems. *J. Cryst. Growth.* **2004**, *263*, 459–465. [CrossRef]
49. Fevotte, G.; Gherras, N.; Moutte, J. Batch cooling solution crystallization of ammonium oxalate in the presence of impurities: Study of solubility, supersaturation, and steady-state inhibition. *Cryst. Growth Des.* **2013**, *13*, 2737–2748. [CrossRef]
50. Kim, J.H.; Park, J.M. Ultrasound-Assisted Micellar Extraction for Paclitaxel Purification from *Taxus chinensis*. *Korean Inst. Chem. Eng.* **2021**, *59*, 106–111. [CrossRef]
51. Min, H.S.; Kim, J.H. Negative pressure cavitation fractional precipitation for the purification of paclitaxel from *Taxus chinensis*. *Korean J. Chem. Eng.* **2022**, *39*, 58–62. [CrossRef]
52. Kang, H.J.; Kim, J.H. Development of an improved acetone-water fractional precipitation process for purification of paclitaxel from *Taxus chinensis* and its kinetic and thermodynamic analysis. *Korean Chem. Eng. Res.* **2021**, *59*, 379–392. [CrossRef]
53. Park, G.Y.; Kim, G.J.; Kim, J.H. Effect of tar compounds on the purification efficiency of paclitaxel from *Taxus chinensis*. *J. Ind. Eng. Chem.* **2015**, *21*, 151–154. [CrossRef]